Pinning and transport of cyclotron (Landau) orbits by electromagnetic vortices

Iwo Bialynicki-Birula*

Center for Theoretical Physics, Polish Academy of Sciences,

Al. Lotników 32/46, 02-668 Warsaw, Poland and

Institute of Theoretical Physics, Warsaw University, Hoża 69, 00-681 Warsaw, Poland

Tomasz Radożycki[†]
Physics Department, Warsaw University, Hoża 74, 00-682 Warsaw, Poland

Electromagnetic waves with phase defects in the form of vortex lines combined with a constant magnetic field are shown to pin down cyclotron orbits (Landau orbits in the quantum mechanical setting) of charged particles at the location of the vortex. This effect manifests itself in classical theory as a trapping of trajectories and in quantum theory as a Gaussian shape of the localized wave functions. Analytic solutions of the Lorentz equation in the classical case and of the Schrödinger or Dirac equations in the quantum case are exhibited that give precise criteria for the localization of the orbits. There is a range of parameters where the localization is destroyed by the parametric resonance. Pinning of orbits allows for their controlled positioning. They can be transported by the motion of the vortex lines.

PACS numbers: 42.50.Vk, 03.65.-w, 45.50.-j, 52.20.Dq

I. INTRODUCTION

The transverse motion of charged particles in a constant magnetic field is fully delocalized. The classical trajectories of particles projected on the plane perpendicular to the field are circles which can be moved around without changing the particle energy. The wave functions of a particle in quantum mechanics exhibit the same behavior. If $\psi(\mathbf{r})$ is a solution of the Schrödinger or the Dirac equation with the energy E, then a shifted wave function $\exp(ie\mathbf{r}\cdot(\mathbf{r}_0\times\mathbf{B})/2\hbar)\psi(\mathbf{r}-\mathbf{r}_0)$ is also a solution with the same energy. In the present paper we shall show that electromagnetic beams with vortex lines localize the classical and quantum states at the position of the vortex and when the vortex line is moved the orbits will follow. In order to describe these properties quantitatively we shall use new exact solutions of the equations of motion obtained in the presence of an electromagnetic field comprising a constant magnetic field and a wave with a vortex line. This paper extends our earlier analysis [1] by adding a constant magnetic field. This extension is significant because the addition of a constant field introduces the third parameter characterizing the electromagnetic field. From the three parameters (the wave frequency and two field amplitudes) we can construct two dimensionless parameters and the space of distinct solutions, as compared to those given in [1], becomes much richer. An extensive analysis of the exact solutions of relativistic equations of motion can be found in a monograph by Bagrov and Gitman [2]. However, they overlooked the existence of the solutions described in this paper. A related problem — the motion of a particle in a constant mag-

*Electronic address: birula@cft.edu.pl †Electronic address: torado@fuw.edu.pl

netic field and a plane electromagnetic wave — has been treated in detail by Roberts and Buchsbaum [3] a long time ago. The crucial difference between these two cases is that the translational symmetry in the plane perpendicular to the magnetic field is broken by the presence of an electromagnetic vortex and the problem becomes truly three-dimensional.

The aim of the present paper is not only to present new analytic solutions of the classical and quantum equations of motion in some realistic configurations of the electromagnetic field but also to describe a universal confining mechanism of charged particles that might have experimental applications. This mechanism acts for all electromagnetic waves with a definite angular momentum. Such waves are characterized by the presence of an electromagnetic vortex. At the vortex the field vanishes and near the vortex the electric and magnetic field vectors exhibit a characteristic behavior that leads to the trapping of particles. The trapping of atoms by electromagnetic vortices is a well established phenomenon [4, 5, 6]. It employs the dipole force pushing atoms in the direction of a decreasing field amplitude in a laser beam that is bluedetuned from the relevant atomic transition. The mechanism for trapping charged particles by electromagnetic vortices is completely different. It employs the rotation of the electric and magnetic field vectors near the vortex

This paper contains a complete, classical, and quantum mechanical description of the motion of charged particles in a combination of an electromagnetic wave with an embedded vortex and a constant magnetic field. Our treatment is fully relativistic but we also present the results in the nonrelativistic limit. In Sec. II we introduce a model electromagnetic wave that approximates very well, near the vortex line, all solutions of Maxwell equations with the lowest angular momentum. In Sec. III we give general solutions of the Lorentz equations in such a wave

and exhibit a mechanism that confines the particle in the vicinity of the vortex line. In Sec. IV we show how trapped particles can be transported by moving vortex lines. In Sec. V we carry our analysis to the quantum theory presenting exact solutions of the Dirac equation in the presence of a wave with a vortex and the magnetic field. Finally, we present solutions of the Schrödinger equation describing the transport of Landau orbits.

II. THE SIMPLEST ELECTROMAGNETIC BEAM WITH A VORTEX LINE

The notion of a vortex line of the electromagnetic field can be traced back to an old paper by Rainich [8]. A detailed analysis with many examples has been recently given by us in Ref. [9]. In this paper we shall use only a very special case of the vortex line — the one that is found in null solutions of the Maxwell equations [10]. In reality, vortex lines of the electromagnetic field are most commonly found in beams carrying angular momentum [11, 12, 13]. Such beams can now be produced with the use of several methods: computer generated holograms, axicons, spatial light modulators, and biaxial crystals, etc.. The best known examples of such beams are the Bessel beams and the exact Laguerre-Gaussian (LG) beams. These are solutions of the Maxwell equations obtained by separating the variables in cylindrical coordinates [14]. A convenient description of these beams in terms of just one complex function is obtained with the use of a complex vector

$$F(r,t) = E(r,t) + icB(r,t), \tag{1}$$

which we named the Riemann-Silberstein (RS) vector [15, 16]. The RS vector obeys the complex form of Maxwell equations

$$\partial_t \mathbf{F}(\mathbf{r}, t) = -ic\nabla \times \mathbf{F}(\mathbf{r}, t), \quad \nabla \cdot \mathbf{F}(\mathbf{r}, t) = 0.$$
 (2)

We shall use a representation of ${\bf F}$ in terms of just one complex function

$$F_x = (\partial_x \partial_z + \frac{i}{c} \partial_y \partial_t) \chi, \tag{3a}$$

$$F_y = (\partial_y \partial_z - \frac{i}{c} \partial_x \partial_t) \chi, \tag{3b}$$

$$F_z = -(\partial_x^2 + \partial_y^2)\chi. \tag{3c}$$

where χ is an arbitrary complex solution of the wave equation

$$\left(\frac{1}{c^2}\partial_t^2 - \Delta\right)\chi(\mathbf{r}, t) = 0. \tag{4}$$

An equivalent representation of the electromagnetic field expressed in terms of two real solutions of the wave equation, instead of a single complex solution of the wave equation, has been given by Whittaker [17]. The functions $\chi(\mathbf{r},t)$ for the Bessel beams and for the Laguerre-Gaussian beams are most easily expressed (cf. [18]) in the

cylindrical coordinates (ρ, ϕ, z) . The Bessel beams are labeled by the following parameters ("quantum numbers"): the transverse wave vector $k_{\perp} = \sqrt{k_x^2 + k_y^2}$, the (dimensionless) angular momentum m, the wave vector k_z in the direction of propagation, and the helicity $\sigma = \pm 1$

$$\chi_B(\rho, \phi, z, t) = e^{-i\sigma(\omega_k t - k_z z - m\phi)} J_m(k_\perp \rho).$$
 (5)

The Laguerre-Gaussian beams are defined as

$$\chi_{LG}(\rho, \phi, z, t) = \frac{e^{-i\sigma(\omega t_- - m\phi)}\rho^m}{a(t_+)^{n+m+1}} \exp\left(-\frac{\rho^2}{a(t_+)}\right) L_n^m \left(\frac{\rho^2}{a(t_+)}\right), \quad (6)$$

where $t_{\pm}=t\pm z/c$ and $a(t_{+})=l^{2}+i\sigma c^{2}t_{+}/\omega$, and L_{n}^{m} is the Laguerre polynomial. The natural number n gives the number of zeros of the polynomial but otherwise has no direct physical meaning. The parameter l determines the transverse size (waist) of the LG beam. In the limit, when $k_{\perp} \rightarrow 0$ for Bessel beams and $l \rightarrow \infty$ for LG beams, both functions (5) and (6) reduce (for m>0 and apart from numerical prefactors) to the same solution of the wave equation

$$\chi(\mathbf{r},t) = (x+iy)^m e^{-i\sigma\omega(t-z/c)}. (7)$$

This choice of χ leads to the following RS vector

$$\mathbf{F}(\mathbf{r},t) = \sigma \left(\hat{\mathbf{x}} + i\hat{\mathbf{y}}\right) (x + iy)^{m-1} e^{-i\sigma\omega(t - z/c)}, \quad (8)$$

where we again disregarded some numerical prefactors. The RS vector (8) is a good approximation to the Laguerre-Gaussian and Bessel beams near the z axis, when $\rho \ll l$ or $\rho k_{\perp} \ll 1$. It belongs to a family of the solutions of the Maxwell equations describing vortex lines riding atop a null electromagnetic field [10].

The simplest solution, the one with a unit vortex strength, is obtained by choosing m=2 in Eq. (8). In this case, the electric and magnetic field vectors are

$$E(\mathbf{r},t) = \sigma B\omega \left(f(\mathbf{r},t), g(\mathbf{r},t), 0 \right), \tag{9a}$$

$$\boldsymbol{B}(\boldsymbol{r},t) = \sigma \frac{B\omega}{c} \left(-g(\boldsymbol{r},t), f(\boldsymbol{r},t), 0 \right), \tag{9b}$$

where we introduced the field amplitude expressed in terms of the magnetic field strength and

$$f(\mathbf{r},t) = x\cos\omega(t - z/c) + \sigma y\sin\omega(t - z/c), \quad (10a)$$

$$g(\mathbf{r}, t) = \sigma x \sin \omega (t - z/c) - y \cos \omega (t - z/c). \tag{10b}$$

This simple, linear dependence of the field vectors on x and y will enable us to find explicit solutions of the equations of motion. The expressions (9) and (10) show that the sign factor σ determines the helicity — the sense of rotation of the pair of vectors \mathbf{E} and \mathbf{B} . At each point this pair of vectors rotates with the wave frequency ω but, in contrast to the circularly polarized plane wave, the orientation is not the same in the whole plane but the pair rotates as we move around the vortex line (see

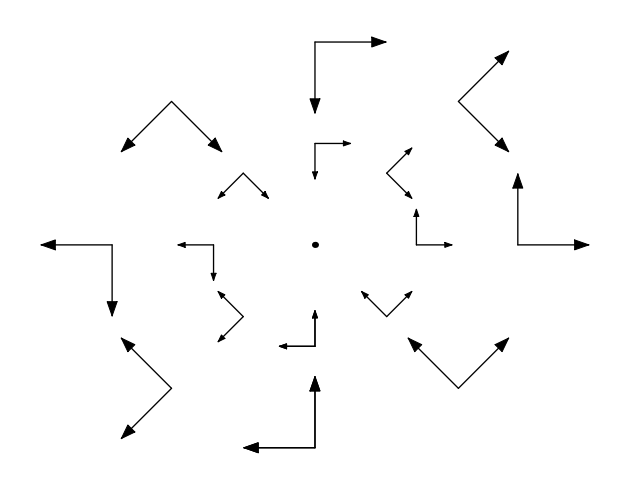


FIG. 1: This figure shows the orientation and also the strength of the electric and magnetic field vectors at t=0 and in the z=0 plane for the solution of the Maxwell equations with a vortex line described by Eq.(9). The point in the middle represents the position of the vortex line. All plots in this paper were generated with the help of MATHEMATICA [7].

Fig. 1). In our case, since the vortex has a unit strength, the full rotation angle is 2π .

We have shown recently [1] that there exist analytic solutions in the classical and quantum theory describing the motion of charged particles in the presence of the electromagnetic beam [Eq.9]. Exact solutions exist because the transverse motion (in the plane perpendicular to the direction of the beam propagation) almost separates from the longitudinal motion. The separation is not complete but the longitudinal motion influences only the values of the integration constant appearing in the equations of motion describing the transverse dynamics. The exact solvability is not destroyed by the presence of an additional constant magnetic field aligned with the beam direction. The presence of this field adds a new dimension to the space of control parameters and significantly enriches the dynamical behavior of the system.

The electromagnetic field (9) may seem unrealistic since its amplitude increases without bound with the growing distance from the z axis. However, we shall show that the particle is often confined to a region close to the z axis and is subject practically the same field as that of much more realistic Laguerre-Gaussian or Bessel beams. This expectation has been recently fully confirmed in [19] where we have shown that numerical solutions of the Lorentz equation in the presence of Bessel beams near the vortex line exhibit the same behavior as the analytic solutions found in [1] for the model wave (9).

III. CLASSICAL MECHANICS

We shall give first a fully relativistic description of the motion because the nonrelativistic approximation can be easily obtained from the relativistic solution by taking the limit $c \to \infty$.

A. Relativistic motion

The Lorentz equations of motion

$$m \ddot{\xi}^{\mu}(\tau) = e f^{\mu\nu} [\xi(\tau)] \dot{\xi}_{\nu}(\tau), \tag{11}$$

that govern the motion of a relativistic particle moving in the presence of the electromagnetic wave [Eq.(9)] and a constant magnetic field $\mathbf{B}_0 = (0, 0, B_0)$, aligned with the beam direction, can be written in the form

$$\ddot{\xi} = \sigma \omega_c \,\omega \, f(\xi, \eta, \zeta, \theta) \left(\dot{\theta} - \dot{\zeta}/c \right) + \omega_0 \dot{\eta}, \tag{12a}$$

$$\ddot{\eta} = \sigma \omega_c \,\omega \,g(\xi, \eta, \zeta, \theta) \left(\dot{\theta} - \dot{\zeta}/c\right) - \omega_0 \dot{\xi},\tag{12b}$$

$$\ddot{\zeta} = \sigma \frac{\omega_c \, \omega}{c} [\dot{\xi} f(\xi, \eta, \zeta, \theta) + \dot{\eta} g(\xi, \eta, \zeta, \theta)], \tag{12c}$$

$$c\ddot{\theta} = \sigma \frac{\omega_c \omega}{c} \dot{\xi} f(\xi, \eta, \zeta, \theta) + \dot{\eta} g(\xi, \eta, \zeta, \theta)],$$
 (12d)

where $\xi(\tau), \eta(\tau), \zeta(\tau)$ are the space components and $\theta(\tau)$ is the time component of the four-vector $\xi^{\mu}(\tau)$. To save space we dropped the dependence on τ . The dots denote derivatives with respect to the proper time τ . The two cyclotron frequencies $\omega_c = eB/m$ and $\omega_0 = eB_0/m$ measure the intensity of the wave and the strength of the constant magnetic field, respectively. They can be either positive or negative. The negative value of ω_0 means the reversal of the magnetic field direction.

From now on, we shall assume that $\sigma=1$ because the equations of motion (12) with the functions f and g defined by Eq.(10) are invariant under the following transformation

$$\sigma \to -\sigma, \ \xi \longleftrightarrow \eta, \ \omega_0 \to -\omega_0.$$
 (13)

Therefore, we do not obtain anything essentially new by considering both signs of σ , since to every trajectory for $\sigma = -1$ there corresponds a trajectory for $\sigma = 1$ in the reversed constant magnetic field, differing only by a reflection with respect to the x = y plane.

The Lorentz equations (12) are nonlinear but they can be effectively linearized owing to conservation laws. In doing so, we shall follow the procedure developed in Ref. [1]. The first constant of motion \mathcal{E} is obtained by subtracting Eq. (12c) from Eq. (12d) which gives $\ddot{\theta} - \ddot{\zeta}/c = 0$ or $\dot{\theta} - \dot{\zeta}/c = \mathrm{const}_1$. Thus, \mathcal{E} is a conserved quantity

$$\mathcal{E} = \dot{\theta} - \dot{\zeta}/c = \sqrt{1 + (\dot{\xi}^2 + \dot{\eta}^2 + \dot{\zeta}^2)/c^2} - \dot{\zeta}/c.$$
 (14)

Apart from the factor mc^2 , the constant \mathcal{E} is the light-front energy — the conjugate variable to $t_+ = t + z/c$

$$\mathcal{E} = \frac{1 - v_z/c}{\sqrt{1 - \mathbf{v}^2/c^2}} = \frac{\sqrt{m^2 c^4 + \mathbf{p}^2 c^2} - p_z c}{mc^2}.$$
 (15)

We shall assume that we start counting the proper time τ in such a way that $\theta(0) - \zeta(0)/c = 0$. Under this assumption, Eq. (14) integrated with respect to τ yields

$$\theta - \zeta/c = \mathcal{E}\,\tau. \tag{16}$$

Hence, the proper time is simply proportional to the light-front variable and this will enable us to separate the transverse motion from the longitudinal motion.

The second constant of motion is obtained by subtracting from Eq. (12c) the sum of Eq. (12a) multiplied by $\dot{\xi}/\mathcal{E}$ and Eq. (12b) multiplied by $\dot{\eta}/\mathcal{E}$. Since the right hand sides cancel, we obtain

$$\dot{\zeta} - \frac{1}{2c\mathcal{E}}(\dot{\xi}^2 + \dot{\eta}^2) = \text{const}_2 = \frac{c}{2}(\frac{1}{\mathcal{E}} - \mathcal{E}). \tag{17}$$

The last expression is obtained by rearranging the formula $1 + (\dot{\xi}^2 + \dot{\eta}^2 + \dot{\zeta}^2)/c^2 = (\mathcal{E} + \dot{\zeta}/c)^2$ obtained from Eq. (14).

Owing to Eq. (14), the longitudinal motion affects the transverse motion only through the value of \mathcal{E} and since it is a constant of motion the equations for ξ and η may be solved first. The integration of Eqs. (12a) and (12b) is made simpler by introducing a complex combination of the coordinates $Z = \xi + i\eta$. The equation of motion for Z obtained from Eqs. (12) reads

$$\ddot{Z} = \omega_c \Omega Z^* e^{i\Omega\tau} - i\omega_0 \dot{Z}, \tag{18}$$

where in addition to the two cyclotron frequencies ω_c and ω_0 associated with the strength of the wave and the constant magnetic field we defined the third frequency Ω — an effective wave frequency as seen by the moving particle. Thus, the dynamics of the particle is governed by the three frequencies

$$\Omega = \omega \mathcal{E}, \quad \omega_c = \frac{eB}{m}, \quad \omega_0 = \frac{eB_0}{m}.$$
(19)

The form $\ddot{Z}e^{-i\Omega\tau/2} = \omega_c\Omega(Ze^{-i\Omega\tau/2})^* - i\omega_0\dot{Z}e^{-i\Omega\tau/2}$ of Eq. (18) suggests a transformation to the frame rotating (in proper time) with the angular velocity $\Omega/2$ around the z-axis. This amounts to replacing ξ and η by the new variables

$$\alpha(\tau) = \xi(\tau)\cos(\Omega\tau/2) + \eta(\tau)\sin(\Omega\tau/2), \tag{20a}$$

$$\beta(\tau) = -\xi(\tau)\sin(\Omega\tau/2) + \eta(\tau)\cos(\Omega\tau/2), \qquad (20b)$$

or in complex notation

$$Z = \xi + i\eta = (\alpha + i\beta)e^{i\Omega\tau/2}.$$
 (21)

Upon substituting this expression into Eq. (18), we get rid of an explicit τ dependence and obtain the following equations with constant coefficients for α and β

$$\ddot{\alpha} = (\Omega^2/4 + \Omega\omega_0/2 + \Omega\omega_c)\alpha + (\Omega + \omega_0)\dot{\beta}, \qquad (22a)$$

$$\ddot{\beta} = (\Omega^2/4 + \Omega\omega_0/2 - \Omega\omega_c)\beta - (\Omega + \omega_0)\dot{\alpha}.$$
 (22b)

The mutual relationships between the three frequencies Ω , ω_c , and ω_0 determine whether the transverse motion is localized near the z axis or is unbounded.

A full description is most easily done in the Hamiltonian formalism. The equations of motion (22) can be obtained from the following Hamiltonian

$$H = \frac{p_{\alpha}^{2} + p_{\beta}^{2}}{2m} + m \frac{(a-b)\alpha^{2} + (a+b)\beta^{2}}{2} - w(\alpha p_{\beta} - \beta p_{\alpha}), \tag{23}$$

where

$$a = \frac{\omega_0^2}{4}, \quad b = \Omega \omega_c, \quad w = \frac{\Omega + \omega_0}{2}.$$
 (24)

This Hamiltonian (for $\omega_0 = 0$) differs by a canonical transformation from the one considered in Ref. [1]. We found this new form of the Hamiltonian more convenient than the previous one. The canonical equations of motion can be written in the following matrix form

$$i\frac{d}{dt}X = X \cdot \hat{M},\tag{25}$$

where

$$X = (\alpha, \beta, p_{\alpha}, p_{\beta}), \qquad (26)$$

and

$$\hat{M} = \begin{pmatrix} 0 & -iw & -im(a-b) & 0\\ iw & 0 & 0 & -im(a+b)\\ i/m & 0 & 0 & -iw\\ 0 & i/m & iw & 0 \end{pmatrix}. \quad (27)$$

We have absorbed i into the definition of the matrix \hat{M} to make its eigenvalues equal to the (real) characteristic frequencies. These are the same equations of motion (only with different values of the coefficients) that govern the dynamics of particles in the mechanical model of the Paul trap [20, 21], Trojan asteroids in the Sun-Jupiter system, and Trojan wave packets of Rydberg electrons in an electromagnetic wave [22] or in a molecule with an electric dipole moment [23]. As a matter of fact, every quadratic Hamiltonian, by an appropriate linear canonical transformation, can be reduced to the form (23).

The characteristic frequencies in the present case are

$$\Omega_{\pm} = \Omega r_{\pm}$$

$$r_{\pm} = \frac{1}{2} \sqrt{(1+\mu)^2 + \mu^2 \pm 4\sqrt{\nu^2 + \mu^2(1+\mu)^2/4}} , \quad (28)$$

where we used Ω as a yardstick to measure all frequencies, i.e.

$$\mu = \omega_0 / \Omega, \quad \nu = \omega_c / \Omega.$$
 (29)

The description of the motion with the use of two dimensionless parameters μ and ν is very convenient because it exhibits a self-similarity inherent in our problem. The dimensionless ratios μ and ν provide a unified description of different physical situations. For example, a particle in a 2.45 GHz microwave oven will show the same behavior as a particle in an optical wave of a 505 nm blue laser provided we increase the amplitude of the wave and the strength of the magnetic field by a factor of 2.4210⁵. An increase or decrease of all three frequencies by the same factor does not change the character of the motion but it results in a decrease or increase of characteristic space and time scales. We shall take this fact into account and express the distances in units of the angular wavelength $\lambda = c/\omega$ and the time in units of an angular period $1/\omega$. These units of length and time are used in all the figures in this paper. In other words, we shall use the units in which $\omega = 1$ and c = 1.

Bounded oscillations occur only when both characteristic frequencies Ω_{\pm} are real and this means that

$$|\nu| < \frac{1}{2} \left| \frac{1}{2} + \mu \right|. \tag{30}$$

The mode amplitudes a_{\pm} and a_{\pm}^{*} (classical counterparts of the annihilation and creation operators) are found by solving the eigenvalue problem for the matrix \hat{M} appearing in Eq. (25)

$$a_{+} = \frac{1}{N_{+}^{1/2}} \left[t_{++} \left(p_{\beta} - \frac{m\Omega s_{-}}{1+\mu} \alpha \right) - i \varepsilon t_{+-} \left(p_{\alpha} + \frac{m\Omega s_{+}}{1+\mu} \beta \right) \right],$$
(31a)
$$a_{-} = \frac{1}{N_{-}^{1/2}} \left[t_{--} \left(p_{\beta} + \frac{m\Omega s_{+}}{1+\mu} \alpha \right) + i \varepsilon t_{-+} \left(p_{\alpha} - \frac{m\Omega s_{-}}{1+\mu} \beta \right) \right],$$
(31b)

where to save space we introduced the following functions of μ and ν

$$s_{\pm} = \sqrt{\nu^2 + \mu^2 (1+\mu)^2/4} \pm \nu,$$
 (32a)

$$t_{+\pm} = \sqrt{(1+\mu)^2 + 2s_{\pm}},$$
 (32b)

$$t_{-\pm} = \sqrt{|(1+\mu)^2 - 2s_{\pm}|},$$
 (32c)

$$\varepsilon = \operatorname{sgn}(1 + \mu), \tag{32d}$$

and the normalization factors are

$$N_{+} = 4m\Omega_{+}(s_{+} + s_{-}). \tag{33}$$

This normalization guarantees that a_{\pm} and a_{\pm}^{*} have the canonical Poisson brackets

$$\{a_{\pm}, a_{+}^{*}\} = -i. \tag{34}$$

The formulas (31) are not valid when $\mu = -1$. However, in this special case the equations of motion (22) describe just two uncoupled harmonic oscillators and the determination of eigenmodes is very simple. The Hamiltonian [Eq.(23)] expressed through the amplitudes a_{\pm} reads

$$H = \Omega_{+} a_{+}^{*} a_{+} - \operatorname{sgn}(1/2 + \mu) \Omega_{-} a_{-}^{*} a_{-}.$$
 (35)

The minus sign in the diagonal form of the Hamiltonian, indicates that for $1/2 + \mu > 0$ the oscillations in the transverse plane are bounded due to the Coriolis force — a characteristic feature of the Paul trap or Trojan asteroids and Trojan electrons. We would like to stress that despite its quadratic form the Hamiltonian of the transverse motion does not correspond to a simple harmonic oscillator in two dimensions because the frequencies of oscillations Ω_{\pm} are not fixed once and for all but they depend on the initial velocities through the parameter \mathcal{E} . The regions of stable motion in the $\mu\nu$ plane are shown in Fig. 2.

FIG. 2: Regions of stability in the $\mu\nu$ plane are shown as two shaded areas. In the area on the left hand side we have a normal harmonic oscillator while in the area on the right hand side we have the Trojan regime — stable oscillations but the Hamiltonian is not positive definite.

The general solution for $\xi(\tau)$ and $\eta(\tau)$ in the laboratory frame is obtained by solving Eq. (22) in terms of eigenmodes and then undoing the rotation in Eq.(20). The final expression for the motion of particles in the plane perpendicular to the vortex line can be compactly written in the same complex form as in [1]

$$\xi(\tau) + i\eta(\tau) = e^{i\Omega\tau/2} \left[(iD\kappa_{+} + A)\sin(\Omega_{+}\tau) - (B\kappa_{-} + iC)\sin(\Omega_{-}\tau) + (iA\kappa_{+} - D)\cos(\Omega_{+}\tau) + (C\kappa_{-} - iB)\cos(\Omega_{-}\tau) \right], \quad (36)$$

but the meaning of A, B, C, D, and κ_{\pm} is now different, namely

$$\kappa_{\pm} = \frac{r_{\pm}^2 + 1/4 + \mu/2 \pm \nu}{(1+\mu)r_{+}},\tag{37}$$

and the constants A, B, C, and D are the following functions of the initial values of the transverse positions and

velocities

$$A = \frac{(1/2 - \kappa_{-}r_{-})\eta_{0} + \dot{\xi}_{0}/\Omega}{r_{+} - r_{-}\kappa_{-}\kappa_{-}},$$
 (38a)

$$B = \frac{(\kappa_{+}/2 - r_{+})\eta_{0} + \kappa_{+}\dot{\xi}_{0}/\Omega}{r_{+} - r_{-}\kappa_{-}\kappa_{+}},$$
 (38b)

$$C = \frac{(1/2 - \kappa_{+} r_{+}) \xi_{0} - \dot{\eta}_{0} / \Omega}{r_{-} - r_{+} \kappa_{-} \kappa_{+}},$$
 (38c)

$$D = \frac{(\kappa_{-}/2 - r_{-})\xi_{0} - \kappa_{-}\dot{\eta}_{0}/\Omega}{r_{-} - r_{+}\kappa_{-}\kappa_{+}}.$$
 (38d)

Having found the solution in the transverse plane, we can now just integrate Eq. (17) to obtain the following formula for the longitudinal motion

$$\zeta(\tau) = \frac{c\tau}{2} (\frac{1}{\mathcal{E}} - \mathcal{E}) + \int_0^{\tau} d\tau \frac{1}{2c\mathcal{E}} (\dot{\xi}^2 + \dot{\eta}^2) + \zeta(0). \quad (39)$$

The integration is cumbersome but elementary and it leads to

$$\zeta(\tau) = \frac{c\tau}{2} \left[\frac{1}{\mathcal{E}} - \mathcal{E} + \frac{(A^2 + D^2) \left((\Omega^2 + 4\Omega_+^2)(1 + \kappa_+^2) - 8\Omega\Omega_+ \kappa_+ \right) + (B^2 + C^2) \left((\Omega^2 + 4\Omega_-^2)(1 + \kappa_-^2) - 8\Omega\Omega_- \kappa_- \right)}{8c^2 \mathcal{E}} \right]$$

$$+ \frac{(1 - \kappa_+^2)(\Omega^2 - 4\Omega_+^2) \left[(D^2 - A^2) \sin(2\Omega_+ \tau) - 2AD(1 - \cos(2\Omega_+ \tau)) \right]}{32c \mathcal{E}\Omega_+}$$

$$+ \frac{(1 - \kappa_-^2)(\Omega^2 - 4\Omega_-^2) \left[(B^2 - C^2) \sin(2\Omega_- \tau) + 2BC(1 - \cos(2\Omega_- \tau)) \right]}{32c \mathcal{E}\Omega_-}$$

$$+ \frac{(\kappa_+ - \kappa_-)(\Omega^2 - 4\Omega_+ \Omega_-) + 2(\kappa_+ \kappa_- - 1)\Omega\Omega_m}{8c \mathcal{E}\Omega_p} \left[(CD - AB) \sin(\Omega_p \tau) - (AC + BD)(1 - \cos(\Omega_p \tau)) \right]$$

$$- \frac{(\kappa_+ + \kappa_-)(\Omega^2 + 4\Omega_+ \Omega_-) - 2(\kappa_+ \kappa_- + 1)\Omega\Omega_p}{8c \mathcal{E}\Omega_m} \left[(CD + AB) \sin(\Omega_m \tau) - (AC - BD)(1 - \cos(\Omega_m \tau)) \right] + \zeta(0),$$

$$(40)$$

where $\Omega_p = \Omega_+ + \Omega_-$ and $\Omega_m = \Omega_+ - \Omega_-$. Thus, the motion in the z direction is a composition of a uniform motion in the proper time τ (not in the laboratory time t) and oscillations with four frequencies $2\Omega_\pm$ and $\Omega_+ \pm \Omega_-$. By a fine tuning of the initial conditions we may cancel the uniform motion completely and leave only the oscillations, but any departure from these special values will cause a uniform drift. The appearance of two additional frequencies $\Omega_+ \pm \Omega_-$ is a new feature that is not found in the absence of the constant magnetic field. Note that the motion in the transverse plane is not completely decoupled from the longitudinal motion because the effective frequency Ω , appearing abundantly in the formula (36), depends (through \mathcal{E}) on the initial velocity in the longitudinal direction.

The presence of stability and instability windows is a manifestation of the parametric resonance. In the region of instability the amplitude of oscillations grows exponentially. This is essentially different as compared to the motion of a charged particle in the circularly polarized plane wave and a constant magnetic field. In that case there appears a standard resonance, i.e. the amplitude grows linearly when the frequency of the driving force (the wave) exactly matches the characteristic frequency of the system (cyclotron frequency). When the circularly polarized wave is replaced by a wave with a vortex, the set of linear inhomogeneous differential equations be-

comes a set of homogeneous equations with periodically varying coefficients. The driving force disappears but the coefficients of the equation become now time dependent and there appears a parametric resonance. Its characteristic features are: The appearance of the whole regions of instability (and not only discrete values as in the case of an ordinary resonance), which shrink to just one point $(\omega_0 = -\omega/2)$ when $\omega_c \to 0$ and an exponential growth of the amplitude in all regions of instability.

Three typical stable three-dimensional relativistic trajectories differing by the choice of initial positions are shown in Fig. 3. The trajectories of a particle projected on the xy plane for different values of the parameters μ and ν are shown in Figs. 4–6. The plots demonstrate that the characteristic shapes of the trajectories are very sensitive to the changes of these parameters.

B. Nonrelativistic limit

The solutions of the equations of motion in the nonrelativistic regime can be obtained from the relativistic ones just by formally taking the limit $c \to \infty$. In this limit, the difference between the proper time and the laboratory time disappears. Also, the wave frequency ω and the effective frequency Ω become equal, because $\mathcal{E}=1$. The motion in the longitudinal direction completely de-

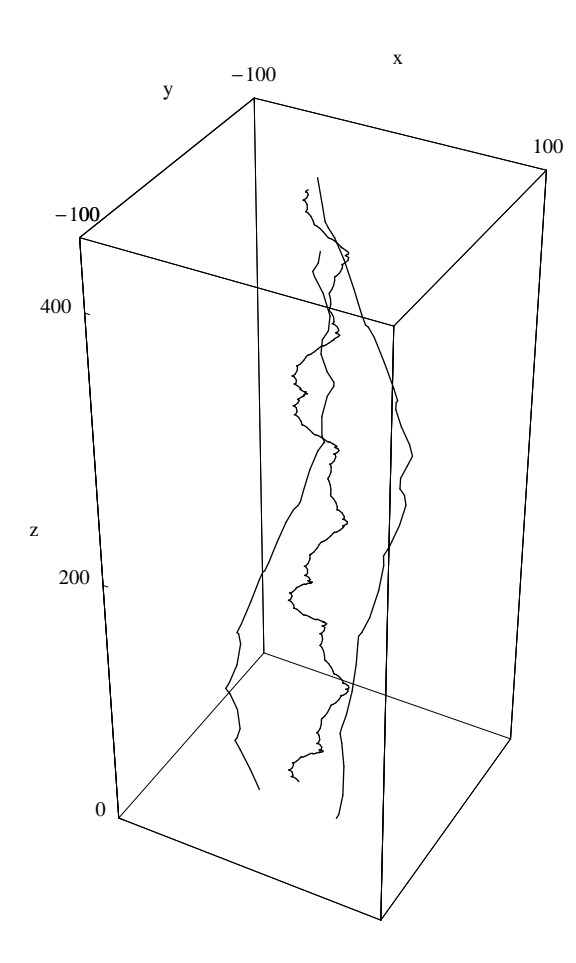


FIG. 3: Three trajectories obtained for $\mu=0.075,\ \nu=0.1,$ and v/c=(0.001,0,0), differing only in the initial positions.

couples from the oscillations in the transverse plane. In the nonrelativistic limit $c(1/\mathcal{E}-\mathcal{E})/2 \to v_z$. In this limit, the motion in the z direction becomes a free motion described by the formula $z(t)=z_0+v_zt$. In contrast to the relativistic case, the velocity in the z direction does not show any oscillations, $v_z=v_{z0}$. We arrive at the same conclusions by solving the nonrelativistic equations of motion $(\sigma=1)$

$$\frac{d^2\xi}{dt^2} = \omega_c \,\omega \,(\xi \cos \omega t + \eta \sin \omega t) + \omega_0 \frac{d\eta}{dt},\tag{41a}$$

$$\frac{d^2\eta}{dt^2} = \omega_c \,\omega \,(\xi \sin \omega t - \eta \cos \omega t) - \omega_0 \frac{d\xi}{dt},\tag{41b}$$

$$\frac{d^2\zeta}{dt^2} = 0, (41c)$$

which are obtained from the Lorentz equations (12) in the limit $c \to \infty$. Since the decoupling of the longitudinal and the transverse motion in the nonrelativistic limit is complete, we may easily obtain in this case also the solutions for a two-dimensional gas of mutually noninteracting charged particles kept near the surface by an additional confining potential V(z).

IV. TRANSPORT OF ORBITS BY MOVING VORTICES

Orbits trapped by vortices can be moved around across the magnetic field. The simplest case is a uniform motion. The electromagnetic field with a moving vortex line can be easily obtained from the field with a stationary vortex line [Eq.(9)] by a Lorentz transformation. Assuming that the motion is along the x axis with velocity v, we obtain the following transformed electric and magnetic field vectors

$$\frac{\mathbf{E}_v}{B\omega} = \begin{pmatrix} \gamma(x - vt)\cos\varphi + y\sin\varphi \\ \gamma^2(x - vt)\sin\varphi - \gamma y\cos\varphi \\ -v(\gamma^2(x - vt)\cos\varphi + \gamma y\sin\varphi)/c \end{pmatrix}, \quad (42a)$$

$$\frac{c\mathbf{B}_{v}}{B\omega} = \begin{pmatrix}
-\gamma(x - vt)\sin\varphi + y\cos\varphi \\
\gamma^{2}(x - vt)\cos\varphi + \gamma y\sin\varphi \\
v(\gamma^{2}(x - vt)\sin\varphi - \gamma y\cos\varphi)/c
\end{pmatrix}, (42b)$$

where $\gamma=1/\sqrt{1-v^2/c^2}$ and $\varphi=\omega[\gamma(t-vx/c^2)-z/c]$. In Fig. 7 we show the trajectory of a particle that is being pulled across the constant magnetic field by the uniformly moving vortex line. Note that this is not the same as transforming the whole problem to a moving frame by a Lorentz transformation. Such a transformation would result also in a change of the constant magnetic field into a crossed magnetic and electric fields.

The transport with a uniform average velocity is just the simplest example, but there is a plethora of more intricate cases, all of them exhibiting the same behavior. The simplest method to construct a solution of the Maxwell equations with a vortex line undergoing complicated motions is to superimpose our basic solution [Eq.(9)] with circularly polarized plane waves moving in the same direction, slightly detuned from the frequency ω . We shall consider here two cases: a superposition with just one plane wave and a superposition with two waves. In the first case, the vortex position at a fixed value of z will move on a circle and in the second case it will follow a trefoil figure.

In the circular case, we shall choose the Riemann-Silberstein vector in the form

$$\mathbf{F}_{c}(\mathbf{r},t) = B\omega \left(\hat{\mathbf{x}} + i\hat{\mathbf{y}}\right)$$

$$\times \left[(x+iy)e^{-i\omega(t-z/c)} - (x_1+iy_1)e^{-i\omega_1(t-z/c)} \right], \quad (43)$$

where x_1 and y_1 are two parameters that fix the radius of the circle and the initial position of the vortex. The vanishing of the RS vector determines the position (x_v, y_v) of the vortex line as a function of z and t

$$x_v(z,t) + iy_v(z,t) = (x_1 + iy_1)e^{i(\omega - \omega_1)(t - z/c)}.$$
 (44)

The vortex forms a screw line of the radius $\sqrt{x_1^2 + y_1^2}$ and the step $2\pi c/(\omega - \omega_1)$ rotating with the angular frequency $\omega - \omega_1$ around the z axis. The formulas for the electric

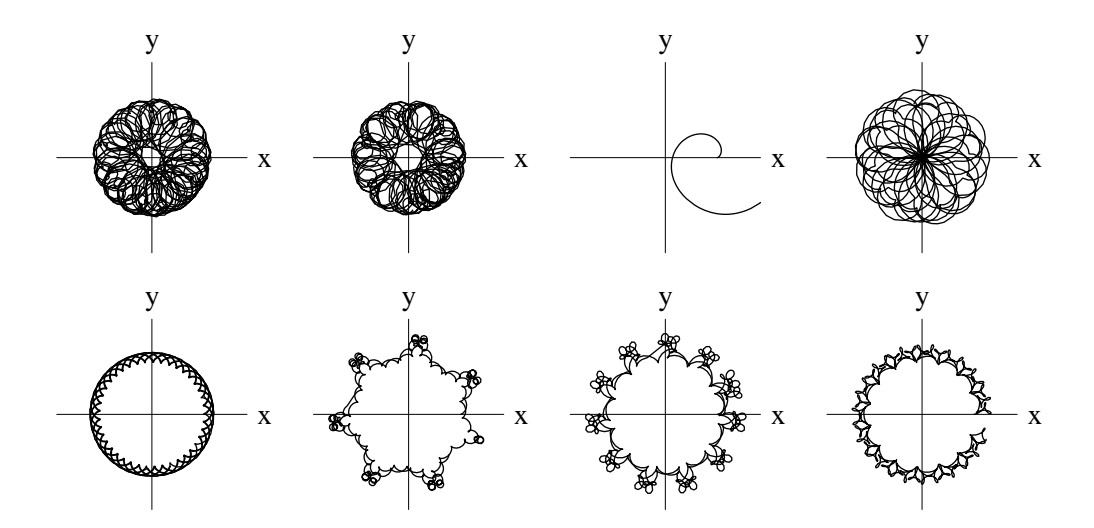


FIG. 4: The trajectories of a particle projected on the xy plane are shown for different values of the parameter μ (i.e. for different values of the constant magnetic field) $\mu = (-0.75, -0.7, -0.5, -0.2, 0.0, 0.1, 0.2, 0.4)$. The value of ν has been fixed at $\nu = 0.075$. The initial values of the position vectors (measured in $\lambda = c/\omega$) and velocity vectors (measured in c) are (60, 0, 0) and (0.001, 0, 0.001), respectively. The size of the area shown in these plots is $100\lambda \times 100\lambda$ and the time lapse is $600/\omega$. The third plot shows the exponential growth of the distance from the vortex line characteristic of the unstable regime.

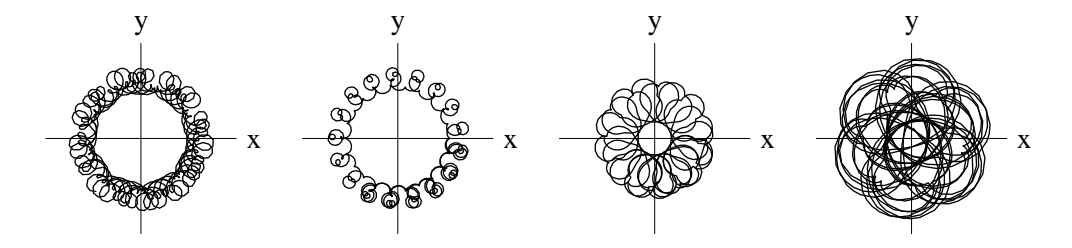


FIG. 5: The trajectories of a particle obtained for the same initial conditions as in Fig. 4. In these plots the value of μ is fixed at $\mu = -0.2$ but the strength of the field amplitude varies as follows: $\nu = (-0.1, -0.05, 0.05, 0.1)$.

and magnetic field vectors read

$$\frac{\boldsymbol{E}_c}{B\omega} = \begin{pmatrix} x\cos\vartheta + y\sin\vartheta - x_1\cos\vartheta_1 - y_1\sin\vartheta_1 \\ x\sin\vartheta - y\cos\vartheta - x_1\sin\vartheta_1 + y_1\cos\vartheta_1 \\ 0 \end{pmatrix}, (45a)$$

$$\frac{c\boldsymbol{B}_c}{B\omega} = \begin{pmatrix} y\cos\vartheta - x\sin\vartheta - y_1\cos\vartheta_1 + x_1\sin\vartheta_1 \\ y\sin\vartheta + x\cos\vartheta - y_1\sin\vartheta_1 - x_1\cos\vartheta_1 \\ 0 \end{pmatrix}, (45b)$$

where $\vartheta = \omega(t-z/c)$ and $\vartheta_1 = \omega_1(t-z/c)$. Thus, the vortex line forms a helix rotating with the angular frequency $\omega - \omega_1$. The projection of this helix on the xy plane forms a circle. In Fig. 8 we show the motion of the particle dragged by such a helical vortex line. The values of the dimensionless parameters $\mu = 0.1$ and $\nu = 0.12$ that determine the character of the motion may correspond to different field and particle configurations. For example, they can describe an electron moving in a constant magnetic field of 1 T and in an electromagnetic microwave of the frequency 2.810^{11} Hz and characteristic intensity 3.410^{10} W/cm². These parameters are not chosen to be very realistic (for example, the intensity is very

high) but they were selected to enhance characteristic features of our solution.

In order to obtain a more elaborate path (a generalized Lissajou figure) of the vortex in the xy plane, we add two plane waves instead of one, i.e.

$$\mathbf{F}_{g}(\mathbf{r},t) = B\omega \,(\hat{\mathbf{x}} + i\hat{\mathbf{y}}) \big[(x+iy)e^{-i\omega(t-z/c)} - (x_1 + iy_1)e^{-i\omega_1(t-z/c)} - (x_2 + iy_2)e^{-i\omega_2(t-z/c)} \big].$$
(46)

In this case, the position of the vortex as a function of t and z is given by the equation

$$x_v(z,t) + iy_v(z,t) = (x_1 + iy_1)e^{i(\omega - \omega_1)(t - z/c)} + (x_2 + iy_2)e^{i(\omega - \omega_2)(t - z/c)}.$$
(47)

The numerical solutions presented here in Figs. 4–9 should leave no doubt that an electromagnetic vortex may easily overcome the inertia of the particle and drag the cyclotron orbit along. Analytic solutions of the equations of motion for a relativistic particle in the presence of electromagnetic waves with moving vortices can also be obtained and they will be described elsewhere.

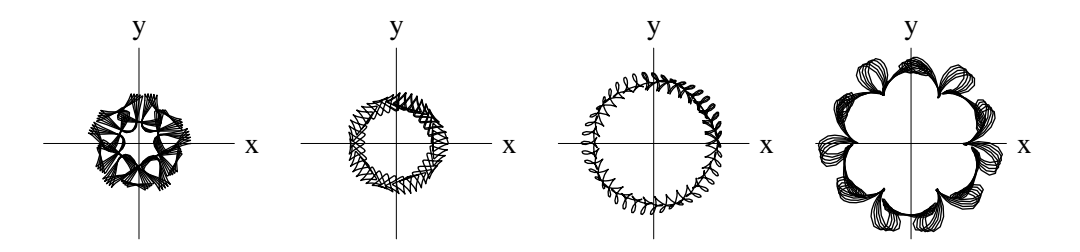


FIG. 6: The trajectories of a particle obtained for the same initial conditions as in Fig. 4. In these plots the value of μ is fixed at $\mu = 0.5$ but the strength of the field amplitude varies as follows $\nu = (-0.2, -0.1, 0.1, 0.2)$.

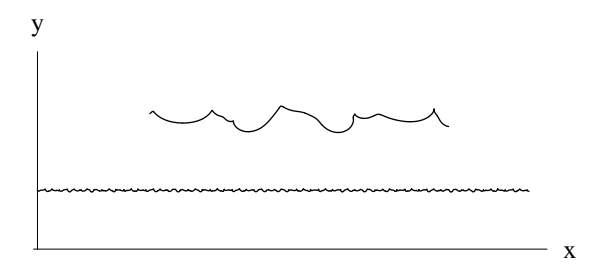
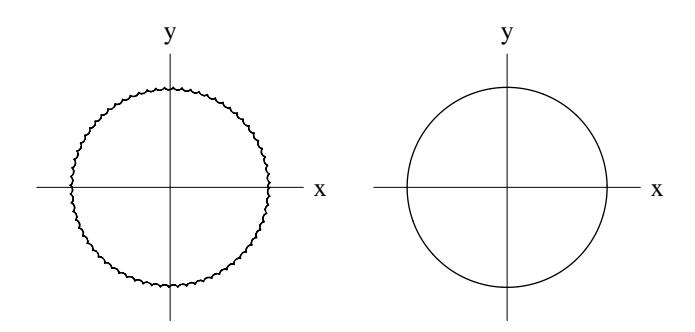


FIG. 7: The transport of an orbit by a moving vortex line. On top of the average motion with a constant velocity in the x direction there are additional oscillations, clearly seen after a tenfold enlargement in the upper part of the figure.



V. QUANTUM MECHANICS

We shall first describe the motion of a quantum particle in the combination of an electromagnetic wave with a vortex line [Eq.(9)] and a constant magnetic field in a fully relativistic case. The nonrelativistic limit will be obtained by a simple reinterpretation of the parameters. Also, the incorporation of spin does not introduce any significant complications. Therefore, we shall start with the Dirac equation.

A. Relativistic quantum mechanics

The Dirac equation for a particle moving in the presence of an electromagnetic field described by a vector potential $\mathbf{A}(\mathbf{r},t)$ can be written in the form

$$i\hbar\partial_t\Psi = \left[c\boldsymbol{\alpha}\cdot(-i\hbar\boldsymbol{\nabla} - e\boldsymbol{A}) + \beta mc^2\right]\Psi.$$
 (48)

In our case, the vector potential can be chosen as

$$\mathbf{A}(\mathbf{r},t) = \begin{pmatrix} -Bg(\mathbf{r},t) - yB_0/2 \\ Bf(\mathbf{r},t) + xB_0/2 \\ 0 \end{pmatrix}. \tag{49}$$

The quantum counterpart of the classical symmetry transformation (13), namely

$$\sigma \to -\sigma, \ x \longleftrightarrow y, \ \omega_0 \to -\omega_0, \ \Psi \to \frac{1 + \alpha_x \alpha_y}{\sqrt{2}} \Psi, \ (50)$$

FIG. 8: The transport of an orbit by a vortex line sweeping out the surface of a cylinder with the radius $10\,\lambda$. The field parameters are $\mu=0.1$ and $\nu=0.12$. The actual particle trajectory (upper plot) is compared with the path that traces the points of the intersection of the vortex line with the xy plane defined by the equation $z=\zeta[\tau]$ (lower plot). The period of the circular motion was chosen as 1000 times the period T of the carrier wave and the time lapse for the trajectory shown in this figure is equal to four full periods of the circular motion. The distances are measured in units of the wavelength $\lambda = c/\omega$ of the carrier wave. Initially the particle was placed at the position of the vortex ($\xi_0 = 10, \eta_0 = 0$) with zero velocity. A slow drift in the z direction is due to relativistic effects.

leaves the Dirac equation invariant. Therefore, we may again restrict ourselves to the case $\sigma=1$ and obtain the solution for $\sigma=-1$ by applying the transformation (50). It is convenient to choose the Dirac representation [24] of α_i and β but with the matrices α_z and β interchanged, i.e.

$$\alpha_x = \rho_x \sigma_x, \ \alpha_y = \rho_x \sigma_y, \ \alpha_z = \rho_z, \ \beta = \rho_x \sigma_z,$$
 (51)

where ρ_i and σ_i are two sets of Pauli matrices acting independently. Next, we split the four component bispinor into two-component wave functions with the help of two projection operators $P_{\pm} = (1 \pm \alpha_z)/2$. In the representation (51), the matrix α_z is diagonal and the splitting amounts to taking the upper and lower components of

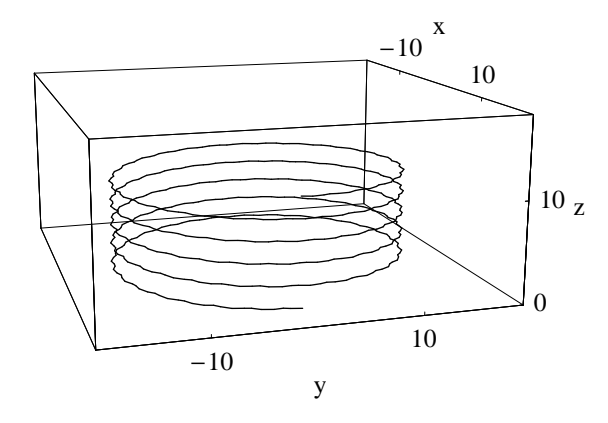


FIG. 9: The transport of an orbit by a vortex line sweeping out a cylindrical surface with the cross section in the form of a trefoil. This figure shows only the projection of the trajectory on the xy plane. The two frequencies in the formula (46) are $1.0005\,\omega$ and $0.999\,\omega$. Since the two detunings are commensurate, the trajectory (right) of the vortex line in the xy plane is closed. The parameters characterizing the position of the vortex are $x_1=5,\,y_1=0,\,x_2=0,$ and $y_2=-10.$ The remaining parameters are $\mu=10$ and $\nu=1.5.$ The distances are measured in units of the wavelength $\lambda=c/\omega$ of the carrier wave. Initially the particle is placed on the vortex line at $\xi_0=5$ and $\eta_0=-10$ with zero velocity. The size of the area in these figures is $20\lambda\times20\lambda$.

the Dirac bispinor Ψ . Therefore, we may write

$$\Psi = P_{+}\Psi + P_{-}\Psi = \begin{pmatrix} \Psi_{+} \\ 0 \end{pmatrix} + \begin{pmatrix} 0 \\ \Psi_{-} \end{pmatrix}$$
 (52)

and the Dirac equation (48) takes on the form

$$2i\hbar\partial_{+}\Psi_{+} = \hat{h}\,\Psi_{-},\tag{53a}$$

$$2i\hbar\partial_{-}\Psi_{-} = \hat{h}\,\Psi_{+},\tag{53b}$$

where $\partial_{\pm} = \partial/\partial t_{\pm} = (\partial_t \pm c\partial_z)/2$ and

$$\hat{h} = c \left[mc\sigma_z - \boldsymbol{\sigma}_{\perp} \cdot (i\hbar \nabla + e\boldsymbol{A}) \right]. \tag{54}$$

From now on, all capitalized Greek letters denote twocomponent spinor wave functions. In the next step, following the procedure of Ref. [1], we perform the transformation to the rotating frame to eliminate the dependence of the potential on t-z/c. To this end, we make the following substitutions in Eqs. (53)

$$\Psi_{\pm} = U\tilde{\Psi}_{\pm} = e^{-i(\omega t_{-}/2\hbar)\hat{M}_{z}}\tilde{\Psi}_{\pm}, \tag{55}$$

where \hat{M}_z is the z component of the total angular momentum

$$\hat{M}_z = \hat{L}_z + \frac{\hbar}{2}\sigma_z = \frac{\hbar}{i}(x\partial_y - y\partial_x) + \frac{\hbar}{2}\sigma_z.$$
 (56)

Under the transformation (55), the z components of all vector operators, r, ∇ , and σ do not change while the x

and y components undergo a rotation, for example,

$$U^{\dagger}xU = x\cos(\omega t_{-}/2) - y\sin(\omega t_{-}/2), \tag{57a}$$

$$U^{\dagger}yU = x\sin(\omega t_{-}/2) + y\cos(\omega t_{-}/2). \tag{57b}$$

Applying these transformations to both Eqs. (53a) and (53b) we obtain

$$2i\hbar\partial_{+}\tilde{\Psi}_{+} = \hat{h}_{0}\tilde{\Psi}_{-}, \tag{58a}$$

$$(2i\hbar\partial_{-} + \omega\hat{M}_z)\tilde{\Psi}_{-} = \hat{h}_0\,\tilde{\Psi}_{+},\tag{58b}$$

where

$$\hat{h}_0 = c \left[mc\sigma_z - \boldsymbol{\sigma}_{\perp} \cdot (i\hbar \nabla + e\boldsymbol{A}_0) \right], \tag{59}$$

and A_0 is the vector potential (49) evaluated at $t_- = 0$,

$$\mathbf{A}_0 = ((B - B_0/2)y, (B + B_0/2)x, 0). \tag{60}$$

Since now there is no explicit dependence on t and z, we may seek solutions of Eqs. (58) by separating these variables

$$\tilde{\Psi}_{\pm}(x, y, z, t) = e^{-i(Et - p_z z)/\hbar} \Phi_{\pm}(x, y), \tag{61}$$

where E and p_z are the separation constants. The equations for $\tilde{\Psi}_{\pm}(x,y)$ have the form

$$(E - p_z c)\Phi_+ = \hat{h}_0 \Phi_-,$$
 (62a)

$$(E + p_z c + \omega \hat{M}_z)\Phi_- = \hat{h}_0 \Phi_+,$$
 (62b)

and upon the elimination of Φ_+ , we obtain the following eigenvalue equation for the transverse motion

$$\left(\frac{(i\hbar\nabla + e\mathbf{A}_0)^2}{2m} - \frac{\hbar\omega_0}{2}\sigma_z - \frac{\Omega}{2}\hat{M}_z\right)\Phi_- = E_\perp\Phi_-, (63)$$

where the energy of the transverse motion is defined as

$$E_{\perp} = \frac{E^2 - m^2 c^4 - (p_z c)^2}{2mc^2} \tag{64}$$

and the effective frequency $\Omega = \mathcal{E}\omega = (E - p_z c)\omega/mc^2$ is the same as in the classical theory [cf. Eq. (15)].

We shall now determine the eigenvalues and the eigenfunctions of the Hamiltonian appearing in (63). Upon the substitution of the explicit form (60) of the vector potential \mathbf{A}_0 , we obtain the following equation

$$\left[-\frac{\hbar^2}{2m} \Delta_{\perp} + \frac{m}{2} \left(\omega_c + \frac{\omega_0}{2} \right)^2 x^2 + \frac{m}{2} \left(\omega_c - \frac{\omega_0}{2} \right)^2 y^2 + i\hbar \omega_c (x\partial_y + y\partial_x) - \frac{\omega_0 + \Omega}{2} \hat{L}_z - \hbar \left(\frac{\omega_0}{2} + \frac{\Omega}{4} \right) \sigma_z \right] \Phi_- = E_{\perp} \Phi_-, \quad (65)$$

where \hat{L}_z is the z component of the orbital angular momentum. This equation, by a substitution

$$\Phi_{-} = e^{im\omega_c xy/\hbar} \Phi, \tag{66}$$

is transformed to the final form

$$\left[-\frac{\hbar^2}{2m} \Delta_{\perp} + \frac{m}{2} \left(\frac{\omega_0^2}{4} - \omega_c \Omega \right) x^2 + \frac{m}{2} \left(\frac{\omega_0^2}{4} + \omega_c \Omega \right) y^2 - \frac{\omega_0 + \Omega}{2} \hat{L}_z - \hbar \left(\frac{\omega_0}{2} + \frac{\Omega}{4} \right) \sigma_z \right] \Phi = E_{\perp} \Phi.$$
(67)

The Hamiltonian in this equation differs only by the spin term from the classical Hamiltonian (23). Since the spin part contributes only an energy shift, we may use the classical amplitudes of normal modes [Eq.(31)] to construct the annihilation operators

$$\hat{a}_{+} = \frac{1}{(\hbar N_{+})^{1/2}} \left[t_{++} \left(\frac{\hbar}{i} \partial_{y} - \frac{m\Omega s_{-}}{1+\mu} x \right) - i\varepsilon t_{+-} \left(\frac{\hbar}{i} \partial_{x} + \frac{m\Omega s_{+}}{1+\mu} y \right) \right], \qquad (68a)$$

$$\hat{a}_{-} = \frac{1}{(\hbar N_{-})^{1/2}} \left[t_{--} \left(\frac{\hbar}{i} \partial_{y} + \frac{m\Omega s_{+}}{1+\mu} x \right) + i\varepsilon t_{-+} \left(\frac{\hbar}{i} \partial_{x} - \frac{m\Omega s_{-}}{1+\mu} y \right) \right]. \qquad (68b)$$

The normalization of these operators is different from their classical counterparts by a factor of $1/\sqrt{\hbar}$ to secure the proper commutation relations. The quantum Hamiltonian, appearing in Eq. (67), expressed in terms of the creation and annihilation operators is (without the spin term)

$$\hat{H} = \hbar \Omega_{+} \hat{a}_{+}^{\dagger} \hat{a}_{+} - \operatorname{sgn}(1/2 + \mu) \hbar \Omega_{-} \hat{a}_{-}^{\dagger} \hat{a}_{-} + \frac{\hbar \Omega_{+}}{2} - \operatorname{sgn}(1/2 + \mu) \frac{\hbar \Omega_{-}}{2},$$
 (69)

where we have used the relations $t_{\pm+}t_{\pm-}=2|1+\mu|\Omega_{\pm}$. It differs from the classical expression (35) by the usual zero-point energy terms.

Now, we shall determine a Gaussian wave function annihilated by the operators \hat{a}_{\pm} . We may do so by substituting a Gaussian wave function in the form

$$\psi_0 = \exp(-q_x x^2/2 - q_y y^2/2 - iqxy) \tag{70}$$

into the equations

$$\hat{a}_{+}\psi_{0} = 0, \quad \hat{a}_{-}\psi_{0} = 0 \tag{71}$$

and find q_x, q_y , and q. By comparing the coefficients at x and y in (71), we obtain the following set of four *linear* equations for the three parameters q_x, q_y and q

$$q_x|1 + \mu|t_{+-} - q(1+\mu)t_{++} = m\Omega s_- t_{++}/\hbar,$$
 (72a)

$$q_y|1 + \mu|t_{++} + q(1+\mu)t_{+-} = m\Omega s_+ t_{+-}/\hbar,$$
 (72b)

$$q_x|1 + \mu|t_{-+} + q(1+\mu)t_{--} = m\Omega s_+ t_{--}/\hbar,$$
 (72c)

$$q_y|1 + \mu|t_{--} - q(1 + \mu)t_{-+} = m\Omega s_- t_{-+}/\hbar.$$
 (72d)

There exists a solution of these equations and it reads

$$q_x = \varpi(s_+ + s_-)t_{++}t_{--},\tag{73a}$$

$$q_y = \varpi(s_+ + s_-)t_{+-}t_{-+},\tag{73b}$$

$$q = \varepsilon \varpi (s_{+}t_{+-}t_{--} - s_{-}t_{++}t_{-+}), \tag{73c}$$

where

$$\varpi = \frac{m\Omega}{\hbar |1 + \mu|(t_{++} + t_{-+} + t_{+-} t_{--})}.$$
 (74)

The parameters q_x, q_y , and q can also be expressed as the following explicit functions of μ and ν

$$q_x = \frac{u}{1 + 2\mu - 4\nu} q_y, (75a)$$

$$q_y = \frac{m\Omega}{4\hbar\sqrt{2\nu^2}}$$

$$\times \sqrt{(1+2\mu-4\nu)[(1+2\mu)(1+\mu)^2-8\nu^2-u]},$$
 (75b)

$$q = \frac{m\Omega}{8\hbar\nu^2}(1 + 2\mu - u),\tag{75c}$$

where $u = \operatorname{sgn}(1/2 + \mu)\sqrt{(1+2\mu)^2 - 16\nu^2}$.

The Gaussian wave function (70) describes an analog of the ground state of the system. This will not always be a true ground state because for $\mu > -1/2$ the Hamiltonian is not positive definite. Having found the state ψ_0 we may generate a complete set ψ_{mn} of "excited" states by acting on ψ_0 with powers of the creation operators

$$\psi_{mn} = \hat{a}_+^{\dagger m} \hat{a}_+^{\dagger n} \psi_0. \tag{76}$$

The wave functions representing these states are Gaussians [Eq.(70)] multiplied by the polynomials in the variables x and y of the (m+n)th order. All wave functions [Eq.(76)] are localized around the vortex line. A complete set of two-component wave functions can be obtained from the one-component functions ψ_{mn} by attaching two independent two-component spinors u_{\pm}

$$\Phi_{mn\pm} = \psi_{mn} u_{\pm}. \tag{77}$$

Choosing the spinors u_{\pm} in the form $u_{+} = (1,0)$ and $u_{-} = (0,1)$ we obtain for each choice of m and n two solutions of the eigenvalue equation (67) of the same shape and differing only in the energy eigenvalues.

Having reduced the problem to a two-dimensional harmonic oscillator, we may use the whole arsenal of tools available in this case. We may combine the classical trajectories with the solutions of the wave equations and construct quantum counterparts of classical motions. Namely, with each pair made of a classical solution of the equations of motion described by the Hamiltonian [Eq.(23)] and a localized wave function [Eq. (76)] we may associate a new solution of the wave equation in the form of a displaced wave function [25, 26, 27] representing a localized wave packet moving along the classical trajectory. These states correspond to coherent states of quantum optics. We may also introduce the analogs of optical squeezed states described by Gaussian wave functions whose shapes are changing during the time evolution. In the next subsection we shall use the Gaussian states to prove that the transport of the orbits by moving vortices, clearly seen in the classical case, carries over to the quantum case.

B. Nonrelativistic quantum mechanics

The eigenvalue equation (63) does not contain the speed of light. Therefore, one may suspect that it coincides with the energy eigenvalue problem for a nonrelativistic charged particle in a coordinate frame rotating with the angular frequency $\Omega/2$. We may confirm this observation by neglecting the relativistic corrections from the very beginning. This amounts to using the nonrelativistic Schrödinger-Pauli equation instead of the Dirac equation

$$i\hbar\partial_t\Psi = \left(\frac{(i\hbar\nabla + e\boldsymbol{A}_{nr})^2}{2m} - \frac{e\hbar}{2m}\boldsymbol{\sigma}\cdot\boldsymbol{B}_0\right)\Psi,$$
 (78)

where in the spirit of the nonrelativistic approximation we have neglected retardation in the expression (49) for the vector potential

$$\mathbf{A}_{nr}(\mathbf{r},t) = \begin{pmatrix} B(y\cos\omega t - x\sin\omega t) - yB_0/2\\ B(x\cos\omega t + y\sin\omega t) + xB_0/2\\ 0 \end{pmatrix}. (79)$$

Note that in the Schrödinger-Pauli equation the magnetic moment is coupled only to B_0 because the magnetic field generated by the vector potential (79) has only the constant part. After the transformation to the rotating

frame we obtain the following eigenvalue equation

$$\left(\frac{(i\hbar\nabla + e\mathbf{A}_0)^2}{2m} - \frac{\hbar\omega_0}{2}\sigma_z - \frac{\omega}{2}\hat{M}_z\right)\Psi = E\Psi. \quad (80)$$

It differs from its relativistic counterpart [Eq. (63)] only by the replacement of the relativistic parameters Ω and E_{\perp} by their nonrelativistic limits ω and E. Thus, the mathematical solutions of the eigenvalue problem obtained in the full relativistic theory can be used, without any modifications, in the nonrelativistic case. This does not mean that the relativistic corrections vanish. They are all contained in a difference between the relativistic parameters (Ω, E_{\perp}) and the nonrelativistic parameters (ω, E) characterizing these solutions.

We shall now apply the time dependent Schrödinger-Pauli equation to the case of a moving vortex to show that the motion of a quantum wave packet corresponds to its classical counterparts. It is convenient to work in the gauge in which the electromagnetic field of the wave is described by the scalar potential. This cannot be achieved for the full electromagnetic field [Eq. (9)] but it can be done in the nonrelativistic approximation, when the retardation effects and the magnetic field of the wave are neglected. In the case of a vortex moving on a circle, the electric field [Eq. (45a)] is obtained from the following scalar potential

$$V(\boldsymbol{r},t) = -eB\omega \left(\frac{x^2 - y^2}{2}\cos(\omega t) + xy\sin(\omega t) - x(x_1\cos(\omega_1 t) + y_1\sin(\omega_1 t)) - y(-y_1\cos(\omega_1 t) + x_1\sin(\omega_1 t))\right). (81)$$

Since the variable z does not appear in the potential, we can separate out the z-dependent part of the wave function and consider only the following Schrödinger-Pauli equation describing the motion in the xy plane

$$i\hbar\partial_t\Psi(x,y,t) = \left(-\frac{\hbar^2}{2m}\Delta_\perp + \frac{m\omega_0^2}{8}(x^2 + y^2) - \frac{\hbar}{2i}\hbar\omega_0(x\partial_y - y\partial_x) + V(x,y,t) - \frac{\hbar\omega_0}{2}\sigma_z\right)\Psi(x,y,t). \tag{82}$$

Upon the transformation to a frame rotating with the angular velocity $\omega/2$, the time dependence in the quadratic part of the Hamiltonian disappears and we obtain an equation for a stationary driven oscillator

$$i\hbar\partial_{t}\Psi(x,y,t) = \left[-\frac{\hbar^{2}}{2m}\Delta + \frac{m\omega_{c}^{2}}{8}(x^{2} + y^{2}) - \frac{\omega_{0} + \omega}{2}\hat{L}_{z} + \omega_{0}\omega\frac{x^{2} - y^{2}}{2} - e\mathbf{r}\cdot\mathbf{E}_{1}(t) - \left(\frac{\hbar\omega_{0}}{2} + \frac{\hbar\omega}{4}\right)\sigma_{z} \right]\Psi(x,y,t), (83)$$

where $E_1(t)$ is the part of the electric field in (45a) with the frequency ω_1 . In the absence of the driving force $E_1(t)$, the Gaussian solution of this equation is given by (70). In order to construct the solution of this equation that corresponds to the classical trajectory shown in Fig. 8 we shall employ a procedure that enables one to obtain from any given solution $\psi_0(\mathbf{r},t)$ of the Schrödinger equation with a quadratic Hamiltonian a family of alternate solutions. These solutions are labeled by all possible classical trajectories and are obtained by "space-shifting" and "phase-shifting" the original solution according to

the formula

$$\psi_{(\xi,\pi)}(\mathbf{r},t) = e^{-iS(t)/\hbar} e^{i\pi_i(t)x^i} e^{-\xi^i(t)\partial_i} \psi_0(\mathbf{r},t), \quad (84)$$

where $\xi^{i}(t)$ and $\pi_{i}(t)$ are the classical positions and momenta and the phase S(t) is the integrated classical action. This construction is based on a generalization of the Dobson's harmonic potential theorem [26]. In the Appendix we give, for completeness, a simple proof of this theorem for the most general quadratic Hamiltonian. We shall consider the simplest case, when ψ_{0} in the rotating frame is given by the Gaussian wave function (70). In

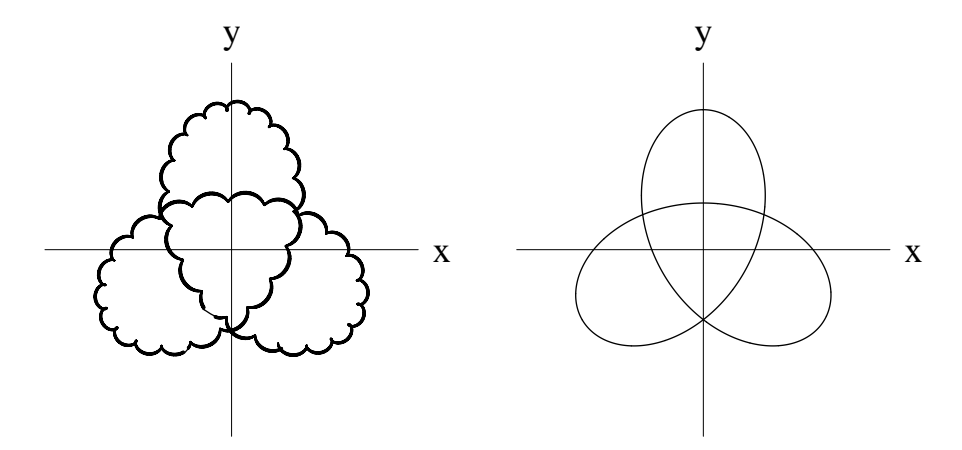


FIG. 10: The transport of a quantum mechanical wave packet in the xy plane by a moving vortex line. Four snapshots of the probability distribution show the wave packet moving along the classical trajectory (superimposed for comparison). The parameters of the classical trajectory are the same as in Fig. 8. The contour lines enclose the areas where the particle is found with the probability 0.1, 0.5, 0.9, and 0.99, correspondingly. Note that due to the influence of the vortex wave the wave packet is squeezed and rotating.

the laboratory frame, the corresponding wave function is obtained by the inverse transformation of the variables as compared to Eq.(57) and it has the form

$$\psi_{L}(\mathbf{r},t) = e^{-q_{x}[x\cos(\omega t/2) + y\sin(\omega t/2)]^{2}/2} \times e^{-q_{y}[y\cos(\omega t/2) - x\sin(\omega t/2)]^{2}/2} \times e^{-iq[x\cos(\omega t/2) + y\sin(\omega t/2)][y\cos(\omega t/2) - x\sin(\omega t/2)]}.$$
 (85)

The new solution corresponding to the classical trajectory depicted in Fig. 8 obtained according to the prescription (84) is

$$\psi_{(\xi,\pi)}(\mathbf{r},t) = e^{-iS(t)/\hbar} e^{-q_x [x\cos(\omega t/2) + y\sin(\omega t/2)]^2/2} \times e^{-q_y [y\cos(\omega t/2) - x\sin(\omega t/2)]^2/2} \times e^{-iq[x\cos(\omega t/2) + y\sin(\omega t/2)][y\cos(\omega t/2) - x\sin(\omega t/2)]}.$$
(86)

In Fig. 10 we show the time evolution of this wave packet, when the center of mass motion is described by the non-relativistic limit of the same classical trajectory that is shown in Fig. 8. The Landau orbit is transported along a circle by the moving vortex. This wave function describes an electron localized with probability 0.99 inside the largest ellipse, transported in the constant magnetic field of by an electromagnetic wave with a moving vortex.

VI. SUMMARY

We have shown that classical (cyclotron) and quantum (Landau) orbits of a charged particle in a constant mag-

netic field can be controlled by electromagnetic waves with embedded vortex lines. These orbits are pinned down in the vicinity of the vortex line and are dragged along when the vortex line moves in the plane perpendicular to the magnetic field. We analyzed this behavior with the use of our new analytic solutions of the Lorentz equations of motion in the classical case and the Dirac (or Schrödinger) wave equation in the quantum case. We show that the trapping of orbits by the vortex in the classical case has its counterpart in the form of Gaussian shape of the wave functions localized in the vicinity of the vortex. The effective reduction of the dynamics of our system to that of a two-dimensional harmonic oscillator makes it possible to give a complete solution using many tools developed in the past for oscillators. In particular, with the use of creation operators we have constructed a complete set of states. Coherent states, the closest analogs of classical orbits, are also easily constructed.

Acknowledgments

We would like to thank and Zofia Bialynicka-Birula, Dmitry Gitman, and Tomasz Sowiński for useful comments and Vladislav Bagrov and Dmitry Gitman for a copy of their book. This research was partly supported by Grant No. 008/P03/2003, Polish Ministry of Science.

APPENDIX A: SOLUTIONS FOR A GENERAL QUADRATIC HAMILTONIAN

In this appendix we show how to construct the new solutions of the Schrödinger equation that were used to describe the transport of Landau orbits. Let us consider the case of the most general quadratic Hamiltonian

$$H(x^{i}, p_{i}, t) = \frac{1}{2} a^{ij}(t) \pi_{i} \pi_{j} + \frac{1}{2} b_{ij}(t) \xi^{i} \xi^{j} + c_{i}^{j}(t) \xi^{i} \pi_{j} - f_{i}(t) \xi^{i} + g^{i}(t) \pi_{i},$$
(A1)

where the summation over repeated indices is understood. The Hamiltonian equations of motion have the form

$$\dot{\xi}^{k}(t) = a^{kj}(t)\pi_{j} + c_{j}^{k}(t)\xi^{j}(t) + g^{k}(t), \quad (A2a)$$

$$\dot{\pi}_k(t) = -b_{kj}(t)\xi^j - c_k^{\ j}(t)\pi_j(t) + f_k(t).$$
 (A2b)

The Schrödinger equation for this system is $(\hbar = 1)$

$$i\partial_t \psi(x^i, t) = \left[-\frac{1}{2} a^{ij}(t) \partial_i \partial_j + \frac{1}{2} b_{ij}(t) x^i x^j - i c_i^j(t) x^i \partial_j, -f_i(t) x^i - i g^i(t) \partial_i + \frac{i}{2} c_i^i \right] \psi(x^i, t).$$
 (A3)

The last term on the right hand side is added to make the quantum Hamiltonian a Hermitian operator. For this system, the following statement holds. For every solution $\psi_0(x^i,t)$ of the Schrödinger equation (A3) without external forces $(f_i = 0 = g^i)$ there corresponds a family of solutions $\psi_{\xi\pi}(x^i,t)$ of the complete equation (A3) obtained by space-shifting and phase-shifting the original solution, namely,

$$\psi_{\xi\pi}(x^i, t) = e^{iS(t)} e^{i\pi_i(t)x^i} \psi_0(x^i - \xi^i(t), t)$$
 (A4)

where $(\xi^i(t), \pi_i(t))$ is any solution of the classical equations of motion (A2). To prove this statement we substitute into (A3) the new wave function written in the form

$$\psi_{\xi\pi}(x^{i}, t) = e^{-iS(t)} U_{\pi} U_{\xi} \psi_{0}(x^{i}, t),$$

$$U_{\pi} = e^{i\pi_{i}(t)x^{i}}, \quad U_{\xi} = e^{-\xi^{i}(t)\partial_{i}}$$
(A5)

and we multiply the whole equation from the left by U_π^{-1} , U_ξ^{-1} , and $e^{-iS(t)}$. Next, we use the relations

$$U_{\pi}^{-1}\partial_{k}U_{\pi} = \partial_{k} + i\pi_{k}(t), \quad U_{\xi}^{-1}x^{k}U_{\xi} = x^{k} + \xi^{k}(t),$$

$$e^{iS(t)}\partial_{t}e^{-iS(t)} = \partial_{t} - i\partial_{t}S(t),$$

$$U_{\pi}^{-1}\partial_{t}U_{\pi} = \partial_{t} + i\dot{\pi}_{i}(t)x^{i}, \quad U_{\varepsilon}^{-1}\partial_{t}U_{\xi} = \partial_{t} - \dot{\xi}^{i}(t)\partial_{i} \quad (A6)$$

and we collect all the terms linear in x^i and ∂_i and independent of x^i and ∂_i . The linear terms cancel due to the classical equations of motion (A2) and the independent terms cancel if the phase S(t) is made equal to the following classical action integral

$$S(t) = \int_0^t dt \left(\frac{1}{2} a^{ij} \pi_i \pi_j - \frac{1}{2} b_{ij} \xi^i \xi^j + g^i \pi_i \right).$$
 (A7)

All remaining terms reduce to the Schrödinger equation satisfied by the wave function $\psi_0(x^i, t)$.

- [1] I. Bialynicki-Birula, Particle Beams Guided by Electromagnetic Vortices: New Solutions of the Lorentz, Schrödinger, Klein-Gordon, and Dirac Equations, Phys.Rev. Lett. 93, 020402 (2004).
- [2] V. G. Bagrov and D. M. Gitman, Exact Solutions of Relativistic Wave Equations, Kluwer, Dordrecht, 1990.
- [3] C. S. Roberts and S. J. Buchsbaum, Motion of a charged particle in a constant magnetic field and a transverse electromagnetic wave propagating along the field, Phys. Rev. 135, A381 (1964).
- [4] J. Arldt, T. Hitomi and K. Dholakia, Atom guiding along Laguerre-Gaussian and Bessel light beams, Appl. Phys. B 71, 549 (2000).
- [5] D. P. Rhodes, D. M. Gherard, J. Livesey, D. McGloin, H. Melville, T. Freegarde and K. Dholakia, Atom guiding along high order Laguerre-Gaussian light beams formed by spatial light modulation, J. Mod. Opt. 53, 547 (2006).
- [6] D. McGloin, G. C. Spalding, H. Melville, W. Sibbett and K. Dholakia, Applications of spatial light modulators in atom optics, Opt. Expr. 11, 158 (2003).
- [7] S. Wolfram, The Mathematica Book, 5th ed, Wolfram Media, Champaign, IL, 2003.
- [8] G. Y. Rainich, Electrodynamics in the general relativity theory, Trans. Am. Math. Soc. 27, 106 (1925).

- [9] I. Bialynicki-Birula and Z. Bialynicka-Birula, Vortex lines of the electromagnetic field, Phys. Rev. A 67, 062114 (2003).
- [10] I. Bialynicki-Birula, Electromagnetic vortices riding atop null solutions of the Maxwell equations, J. Opt. A: Pure Appl. Opt. 6 (2004) S181.
- [11] M. S. Soskin, V. N. Gorshkov, M. V. Vasnetsov, J. T. Malos and N. R. Heckenberg, Topological charge and angular momentum of light beams carrying optical vortices Phys. Rev. A 56, 4064 (1997).
- [12] L. Allen, M. J. Padgett and M. Babiker, The orbital angular momentum of light, Progress in Optics, Vol. 39, edited by E. Wolf, Elsevier, Amsterdam, 1999.
- [13] D. McGloin and K. Dholakia, Bessel beams: diffraction in a new light, Contemp. Phys. 45, 15 (2005).
- [14] J. Stratton, Electromagnetic Theory, McGraw-Hill, New York, 1941, Ch. VI.
- [15] I. Bialynicki-Birula, Photon wave function in Progress in Optics, edited by E. Wolf Elsevier, Amsterdam, 1996; arXiv:/quant-ph/0508202.
- [16] O. Keller, On the theory of spatial localization of photons, Phys. Rep. 411, 1 (2005).
- [17] E. T. Whittaker, On an expression of the electromagnetic field due to electrons by means of two scalar potential

- functions, Proc. Lond. Math. Soc. 1 (1904) 367.
- [18] I. Bialynicki-Birula and Z. Bialynicka-Birula, Beams of electromagnetic field carrying angular momentum: The Riemann-Silberstein vector and the classicalquantum correspondence, Opt. Comm. in print; arXiv:/physics/0502025.
- [19] I. Bialynicki-Birula, Z. Bialynicka-Birula and B. Chmura, Trojan states of electrons guided by electromagnetic vortices, Laser Physics 15, 1371 (2005); arXiv: physics/0309112.
- [20] W. Paul, Electromagnetic traps for charged and neutral particles, Rev. Mod. Phys. 62, 531 (1990).
- [21] I. Bialynicki-Birula and T. Sowiński, Gravity-induced resonances in a rotating trap, Phys. Rev. A 71, 043610 (2005); arXiv:/quant-ph/0412004.
- [22] I. Bialynicki-Birula, M. Kalinski and J. H. Eberly, Lagrange equilibrium points in celestial mechanics and nonspreading wave packets for strongly driven Rydberg elec-

- trons, Phys. Rev. Lett. 73, 1777 (1994).
- [23] I. Bialynicki-Birula and Z. Bialynicka-Birula, Nonspreading wave packets for Rydberg electrons in rotating molecules with electric dipole moments, Phys. Rev. Lett. 77, 4298 (1996).
- [24] P. A. M. Dirac, Principles of Quantum Mechanics, Oxford University Press, Oxford, 1958.
- [25] W. Kohn, Cyclotron resonance and de Haas-van Alphen oscillations of an interacting electron gas, Phys. Rev. 123, 1242 (1961).
- [26] J. F. Dobson, Harmonic-potential theorem: Implications for approximate many-body theories, Phys. Rev. Lett. 73, 2244 (1994).
- [27] I. Bialynicki-Birula and Z. Bialynicka-Birula, Center-ofmass motion in the many-body theory of Bose-Einstein condensates, Phys. Rev. A 65, 63606 (2002).